JGR Atmospheres

RESEARCH ARTICLE
10.1029/2025JD043927

Rapid Recharge and Descent of Thundercloud Core Producing Gamma-Ray Glow

Y. Wada[1], T. Wu[2], M. Kamogawa[3], D. Wang[2], G. Okada[4], H. Nanto[4], T. Sawano[5], M. Kubo[6], D. Yonetoku[7], G. S. Diniz[8], and H. Tsuchiya[9]

[1]Division of Electrical, Electronic and Infocommunications Engineering, Graduate School of Engineering, The University of Osaka, Osaka, Japan, [2]Department of Electrical, Electronic and Computer Engineering, Gifu University, Gifu, Japan, [3]Natural Disaster Research Section, Global Center for Asian and Regional Research, University of Shizuoka, Shizuoka, Japan, [4]Co-creative Research Center of Industrial Science and Technology (CIST), Kanazawa Institute of Technology, Hakusan, Japan, [5]Advanced Research Center for Space Science and Technology, Institute of Science and Engineering, Kanazawa University, Kanazawa, Japan, [6]Faculty of Frontier Engineering, Institute of Science and Engineering, Kanazawa University, Kanazawa, Japan, [7]School of Mathematics and Physics, College of Science and Engineering, Kanazawa University, Kanazawa, Japan, [8]Earth Science System Center (CCST), National Institute for Space Research (INPE), São José dos Campos, Brazil, [9]Nuclear Science and Engineering Center, Japan Atomic Energy Agency, Ibaraki, Japan

Key Points:

- Two gamma-ray glows were tracked by four radiation detectors
- Two glows occurred in an identical region of a collapsing thundercloud and the first terminated with lightning
- The second glow seems to have been associated with a recovery of the electric field by descent of a thundercloud core

Correspondence to:
Y. Wada,
wada@yuuki-wd.space

Citation:
Wada, Y., Wu, T., Kamogawa, M., Wang, D., Okada, G., Nanto, H., et al. (2025). Rapid recharge and descent of thundercloud core producing gamma-ray glow. *Journal of Geophysical Research: Atmospheres*, *130*, e2025JD043927. https://doi.org/10.1029/2025JD043927

Received 20 MAR 2025
Accepted 2 DEC 2025

Author Contributions:
Conceptualization: Y. Wada
Data curation: Y. Wada, T. Wu, D. Wang
Formal analysis: Y. Wada, T. Wu, D. Wang
Funding acquisition: Y. Wada, G. S. Diniz, H. Tsuchiya
Investigation: Y. Wada, T. Wu, D. Wang, G. S. Diniz, H. Tsuchiya
Methodology: Y. Wada, T. Wu, M. Kamogawa, D. Wang, H. Tsuchiya
Project administration: Y. Wada
Resources: Y. Wada, T. Wu, M. Kamogawa, D. Wang, G. Okada, H. Nanto, T. Sawano, M. Kubo, D. Yonetoku
Software: Y. Wada, T. Wu
Supervision: Y. Wada
Validation: Y. Wada, M. Kamogawa, G. S. Diniz, H. Tsuchiya
Visualization: Y. Wada
Writing – original draft: Y. Wada
Writing – review & editing: T. Wu, M. Kamogawa, D. Wang, G. S. Diniz, H. Tsuchiya

Abstract We report two gamma-ray glows observed on 22 December 2023, during a winter thunderstorm in Japan, using an array of four radiation detectors. The first glow, detected by one sensor, was quenched by a lightning discharge. The second glow appeared 2–3 min later and was tracked by three other detectors. Radar observations suggest both glows originated from the same thundercloud cell. However, the detection timing of the second glow was inconsistent with simple thundercloud movement, indicating temporal variations in intrinsic glow brightness. A three-dimensional lightning mapping observation suggests that a discharge activity depleted the electric field that generated the first glow and that the electric field having produced the second glow has been rapidly recovered. In addition, the radar observations also detected a descent of the thundercloud core between the two glows, which may have developed an electrified region and the second glow enough to be observed by the detectors. Tracking gamma-ray glows is crucial for understanding electrified regions in thunderclouds and associated gamma-ray glows.

Plain Language Summary Gamma-ray glows are second-to-minute-duration high-energy emissions from thunderclouds. Electrons are thought to be accelerated and multiplied by electric fields inside thunderclouds and produce high-energy photons by bremsstrahlung. We observed two successive gamma-ray glows by an array of four radiation detectors. The first glow terminated with a lightning discharge, and the second one was detected with three sensors 2–3 min after the termination of the first glow. The tracking observation of the second glow with three sensors was inconsistent with a picture that a gamma-ray glow moves with a thundercloud with a constant brightness. Combining the gamma-ray observations with radar observations, the second glow is suggested to have rapidly developed after the lightning discharge associated with a descent of a thundercloud core.

1. Introduction

Thunderclouds are known to produce high-energy atmospheric phenomena, such as gamma-ray glows. Gamma-ray glows, also known as long bursts (Torii et al., 2002, 2011; Tsuchiya et al., 2007, 2011, 2013) and thunderstorm ground enhancements (TGEs: Chilingarian et al., 2010, 2019; Chum et al., 2020; Kudela et al., 2017), are bursts of high-energy photons emitted from thunderclouds reaching several to tens of MeVs and typically lasting seconds to minutes (Chilingarian et al., 2019; Kochkin et al., 2017; Tsuchiya et al., 2011; Wada, Matsumoto, et al., 2021). The observational studies using aircraft (Kelley et al., 2015; Kochkin et al., 2017, 2021; Marisaldi et al., 2024; McCarthy & Parks, 1985; Østgaard et al., 2019; Parks et al., 1981), balloon (Eack & Beasley, 2015; Eack et al., 1996, 2000), and ground-based experiments (Chilingarian et al., 2010, 2019; Chum et al., 2020; Kudela et al., 2017; Kuroda et al., 2016; Torii et al., 2002, 2011; Tsuchiya et al., 2007, 2011, 2013; Tsurumi et al., 2023; Wada, Enoto, et al., 2021; Wada et al., 2018; Wada, Matsumoto, et al., 2021) have suggested that gamma-ray glows originate from relativistic electrons accelerated and multiplied in highly electrified thundercloud regions with bremsstrahlung occurring from collisions with atmospheric nuclei. The relativistic runaway electron avalanche (RREA: A. Gurevich et al., 1992; A. V. Gurevich & Zybin, 2001; Dwyer, 2003) and the modification of

the cosmic-ray spectrum (MOS: Chilingarian et al., 2012, 2014; Cramer et al., 2017) schemes have been proposed for the acceleration and multiplication processes of electrons in the dense atmospheres. More efficient multiplication processes such as the relativistic feedback scheme may be required for brighter gamma-ray glows (Dwyer, 2003, 2012; Kelley et al., 2015; Wada et al., 2019).

One of the biggest problems for gamma-ray glows is their life cycle; it is not well understood how a gamma-ray glow starts, develops, and ends. The region where electron acceleration occurs, which is the source of gamma-ray glows, is associated with strong electric fields and hence with charge accumulations inside thunderclouds (Chilingarian & Mkrtchyan, 2012; Wada, Enoto, et al., 2021; E. Williams et al., 2022). Therefore, the life cycle of gamma-ray glows can be linked to the charging process of thunderclouds and the development of thundercloud cells. The only clearly observed part of the life cycle is the termination by lightning discharges (Chilingarian et al., 2017, 2020; Kelley et al., 2015; Tsuchiya et al., 2013; Tsurumi et al., 2023; Wada et al., 2018, 2019; Wada, Wu, et al., 2023). This occurs when strong electric-field regions accelerating electrons in the thunderclouds are neutralized by lightning discharges and the acceleration ends. In recent years, lightning discharges associated with glow terminations have been monitored in the radio-frequency band. Two-dimensional or three-dimensional lightning observations lead to discussions on the type and process of lightning discharges, charge distributions inside thunderstorms, and the relation between lightning initiations and glows (Hisadomi et al., 2021; Tsurumi et al., 2023; Wada et al., 2018, 2019; Wada, Wu, et al., 2023). In addition, tracking observations using multiple detectors have revealed that gamma-ray glows move along with thunderclouds (Torii et al., 2011; Tsurumi et al., 2023; Wada et al., 2019; Yuasa et al., 2020).

Winter thunderstorms frequently occur along the coast of the Sea of Japan (Brook et al., 1982; Kitagawa, 1992; Kitagawa & Michimoto, 1994; Michimoto, 1991, 1993). Gamma-ray glows can be detected at sea-level in winter thunderstorms because they have a lower charge center than summer ones, and hence gamma rays are less attenuated before reaching the ground. In contrast, glow observations in summer thunderstorms are limited to aircraft, balloon, and high-altitude experiments. To investigate the life cycle of gamma-ray glows, it is necessary to track a gamma-ray glow for several kilometers by multiple detectors or a mobile detector. Although attempted recently with an aircraft (Marisaldi et al., 2024), tracking observations of gamma-ray glows by aircraft and balloons are technically and financially challenging. High-altitude experiments are more feasible for the tracking observations but are still subject to some constraints such as power sources and location conditions.

The Hokuriku region facing the Sea of Japan is an ideal experimental site as an observation network can be built in urban areas where power sources are secured. In fact, several groups have developed observation networks aiming at winter thunderstorms and succeeded in detecting gamma-ray glows with multiple points (Hisadomi et al., 2021; Torii et al., 2011; Tsurumi et al., 2023; Wada et al., 2019; Yuasa et al., 2020). In this paper, we report a tracking observation of gamma-ray glows with an observation network in Kanazawa, one of the urban areas in the Hokuriku region. The life cycle of the gamma-ray glows is discussed based on radar, radio-frequency, and surface electric-field observations. Hereafter, time is described in the Coordinated Universal Time (UTC) unless otherwise noted.

2. Observation

We are operating an observation network in Kanazawa aiming to detect gamma-ray glows in winter thunderstorms (Yuasa et al., 2020). Since November 2020, six radiation detectors have been deployed in an east-west direction as shown in Figure 1. Winter thunderclouds around Kanazawa typically move with westerly or west-southwest winds (Wada, Matsumoto, et al., 2021; Wada, Tsurumi, et al., 2023), and hence it is possible to track gamma-ray glows by multiple detectors arranged in an east-west direction. Detectors A, B, C, and D are installed on the roofs of Kanazawa Institute of Technology Nonoichi Campus (N36.531°, E136.629°), Kanazawa Izumigaoka High School (N36.538°, E136.649°), Kanazawa Nisui High School (N36.541°, E136.658°), and Kanazawa University High School (N36.539°, E136.664°), respectively. Detectors E and F are installed at two locations (N36.544°, E136.705° and N36.546°, E136.709°) on the Kakuma Campus of Kanazawa University (Wada, Kamogawa, et al., 2023). Each radiation detector is equipped with a 25 × 8 × 2.5-cm bismuth germanate ($Bi_4Ge_3O_{12}$: BGO) scintillator (Yuasa et al., 2020). It means that all the radiation detectors have the same detection efficiency to photons. The energy range is set to 0.4–20 MeV. In the present analysis, we only utilize the energy range above 3 MeV. The range above 3 MeV is dominated by secondary cosmic-ray components and does not show major fluctuations due to washout of radon series such as ^{214}Bi.

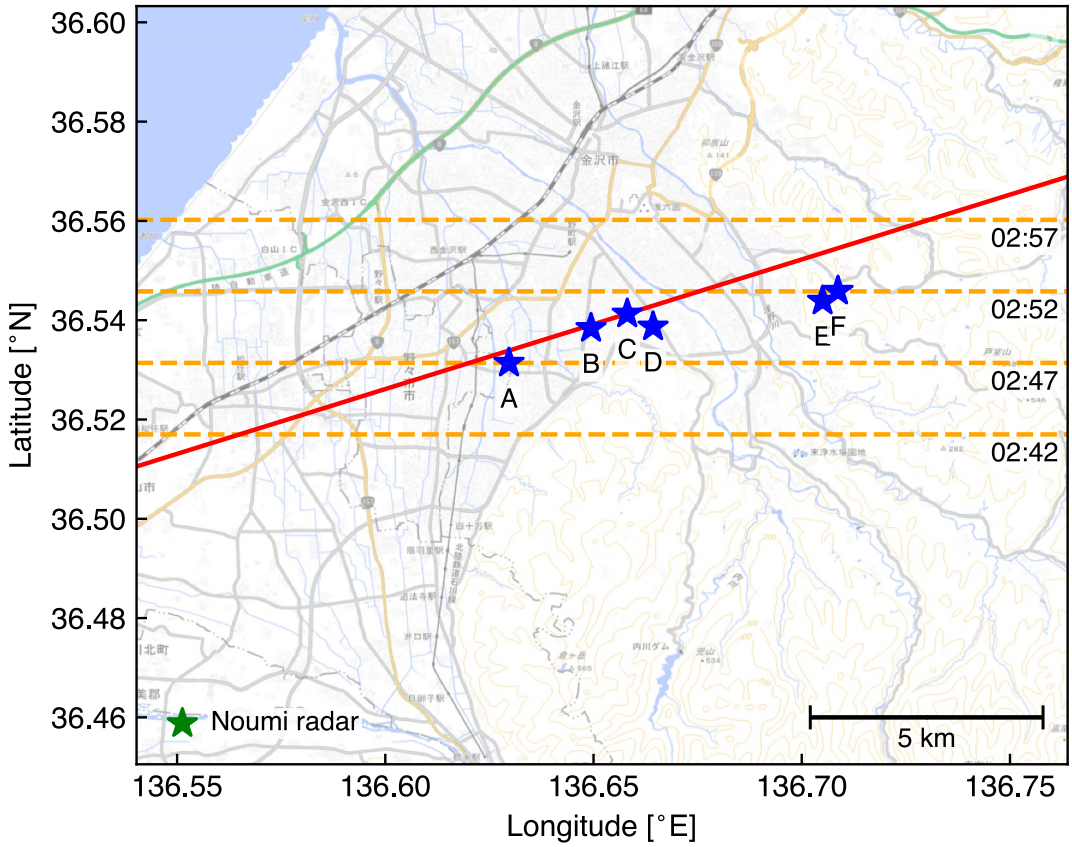

Figure 1. A map of Kanazawa. Blue stars show the location of radiation detectors. The green star shows the location of the Noumi X-band radar site. The red-solid line shows a possible trajectory of the gamma-ray glow moving with a thundercloud. The orange-dashed lines show the position of east-west cross sections of radar observations in Figure 4. The background image is provided by the Geospatial Information Authority of Japan.

Detectors B and D are also equipped with electric-field monitors (field mills Boltek EFM-100) to measure surface electric fields. Plane-surface calibration has not been performed, and only relative values of surface electric fields can be obtained. The field mills are mounted facing upwards and can be affected by charges of precipitation particles.

We utilize the Noumi radar to observe thunderstorms. The Noumi radar is an X-band (9.785 GHz) dual-polarized meteorological radar with a beam width of 1.2°, installed southwest of Kanazawa (N36.459°, E136.551°), and is a part of the eXtended RAdar Information Network (XRAIN) operated by the Ministry of Land, Infrastructure, Transport and Tourism. The Noumi radar completes 30 plan-position indicator (PPI) scans covering 12 elevation angles in 10 min; it observes low elevation angles (1.7° and 3.6°) five times, whereas the other 10 angles (1.0°, 2.6°, 4.8°, 6.1°, 7.5°, 9.0°, 10.6°, 12.3°, 14.1°, and 16.0°) are observed twice. Therefore, a volume scan is compteted within 5 min. The 3.6° elevation angle corresponds to an altitude of 670 m above Detector A. Attenuation correction for reflectivity is applied based on the dual-polarization parameters (Maesaka et al., 2011).

Lightning discharges around Kanazawa are monitored by the fast antenna lightning mapping array (FALMA: Wu et al. (2018)) and the discone antenna lightning mapping array (DALMA: Wang et al., 2022), both operated by Gifu University. FALMA is an observation network using fast antennas, with 14 stations recording the broadband low-frequency (LF) band below 500 kHz. DALMA is an observation network using discone antennas, with 12 stations recording the medium- to high-frequency bands below 12 MHz. By applying the time-of-arrival method, FALMA and DALMA can locate the source of radio-frequency pulses associated with lightning discharges in two dimensions and three dimensions, respectively. In this paper, we mainly use the 3D location results of DALMA, and also refer to the LF waveforms recorded by FALMA stations.

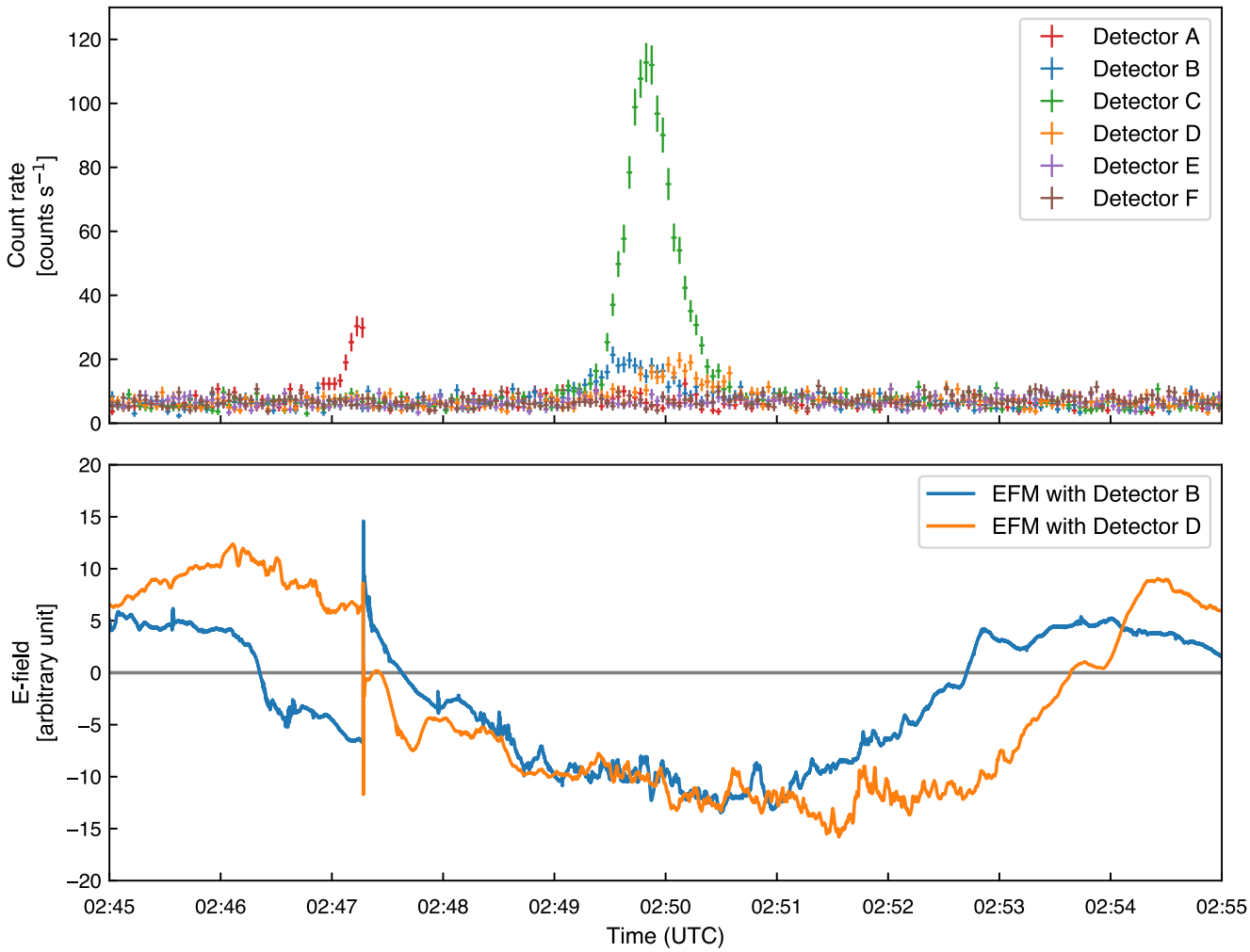

Figure 2. Count-rate histories above 3 MeV recorded by radiation detectors (upper) and surface electric fields recorded by field mills (lower). EFM stands for electric-field monitor or field mills. The field mills are not plane-surface calibrated and only relative values of surface electric fields are available.

3. Results

From 02:46 to 02:51 UTC on 22 December 2023 (11:46–11:51 Japan Standard Time: JST/UTC+9), multiple radiation detectors recorded gamma-ray glows. Figure 2 shows a count-rate history recorded by the radiation detectors with the energy range above 3 MeV. First, Detector A, installed at the westernmost location, detected a gamma-ray glow around 02:47. This gamma-ray glow shows a sudden decrease in count rates to the background level at 02:47:16. From 02:49 to 02:51, Detectors B, C, and D, located east of Detector A, detected another gamma-ray glow. The peak count rate was highest in Detector C, whereas Detector B recorded a similar peak to Detector D. The peak time is determined by fitting the count-rate histories with a Gaussian function to be 02:49:42.6 ± 1.6 s, 02:49:51.1 ± 0.5 s, and 02:50:08.4 ± 1.6 s for Detectors B, C, and D, respectively. No gamma-ray glows were recorded by Detectors E and F around this period.

The lower panel of Figure 2 shows the surface electric fields measured by the field mills beside Detectors B and D. We employ the sign convention of atmospheric electricity for the polarity of electric field; the polarity of the electric field is positive (negative) when a downward (upward) electric field is applied between the ground and the thundercloud. At the moment when the gamma-ray glow recorded by Detector A suddenly terminated both field mills recorded a steep change in the electric fields. This is caused by a lightning discharge, and hence the gamma-ray glow is categorized to be the lightning-terminated type (Wada, Matsumoto, et al., 2021). Before the lightning discharge, the electric field at Detector B was negative, while that at Detector D was positive. At the moment of the lightning discharge, the electric field at Detector B changed from negative to positive, and that at Detector D

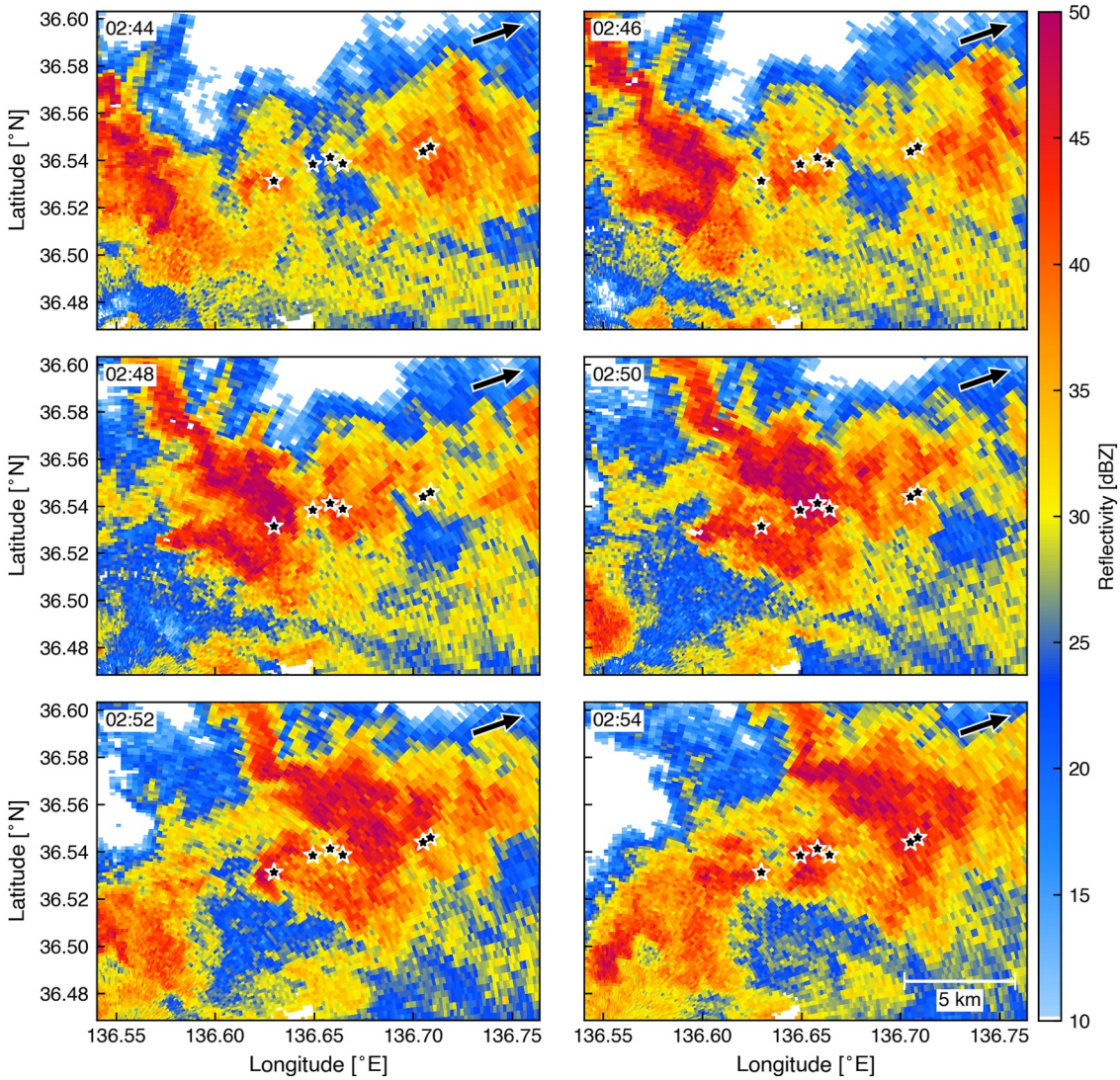

Figure 3. Plan-position indicator (PPI) scans of reflectivity at an elevation angle of 3.6° obtained by the Noumi X-band radar. The black stars show the position of the radiation detectors. The radar echoes moved from west-southwest to east-northeast, and the direction is indicated by the black arrows.

changed from positive to near zero by the lightning discharge. Then, both field mills recorded negative electric fields during the gamma-ray glow recorded by Detectors B–D, whereas the negative peaks of the surface electric fields did not correspond to the count-rate peaks recorded by Detectors B and D. This is consistent with our previous report (Wada, Kamogawa, et al., 2023).

Figure 3 shows PPI scans of reflectivity by the Noumi X-band radar with an elevation angle of 3.6°. From 02:48 to 02:50, a developed radar echo exceeding 40 dBZ, corresponding to a thundercloud, passed above the detector network. The PPI scans are utilized to derive the moving speed of the radar echo. First, PPI scans at an elevation angle of 3.6°, conducted on even minutes, are converted into a 250-m mesh Cartesian coordinate system. Using a 10-km square area centered 14 km northeast of the radar site (around Detector C) as a template, pattern matching is performed to maximize the correlation of reflectivity at four-minutes interval, and the speed and direction of the echo over a four-minute period is estimated. This process is performed on four pairs of six data points from 02:40 to 02:50, and the statistical error is taken as the standard deviation of the four pairs. The systematic error is determined by the mesh size of the Cartesian coordinate system and the data interval used for pattern matching. The estimated speed and direction of the radar echo are 16.7 ± 1.5 m s^{-1} and 250° (north is 0° and clockwise),

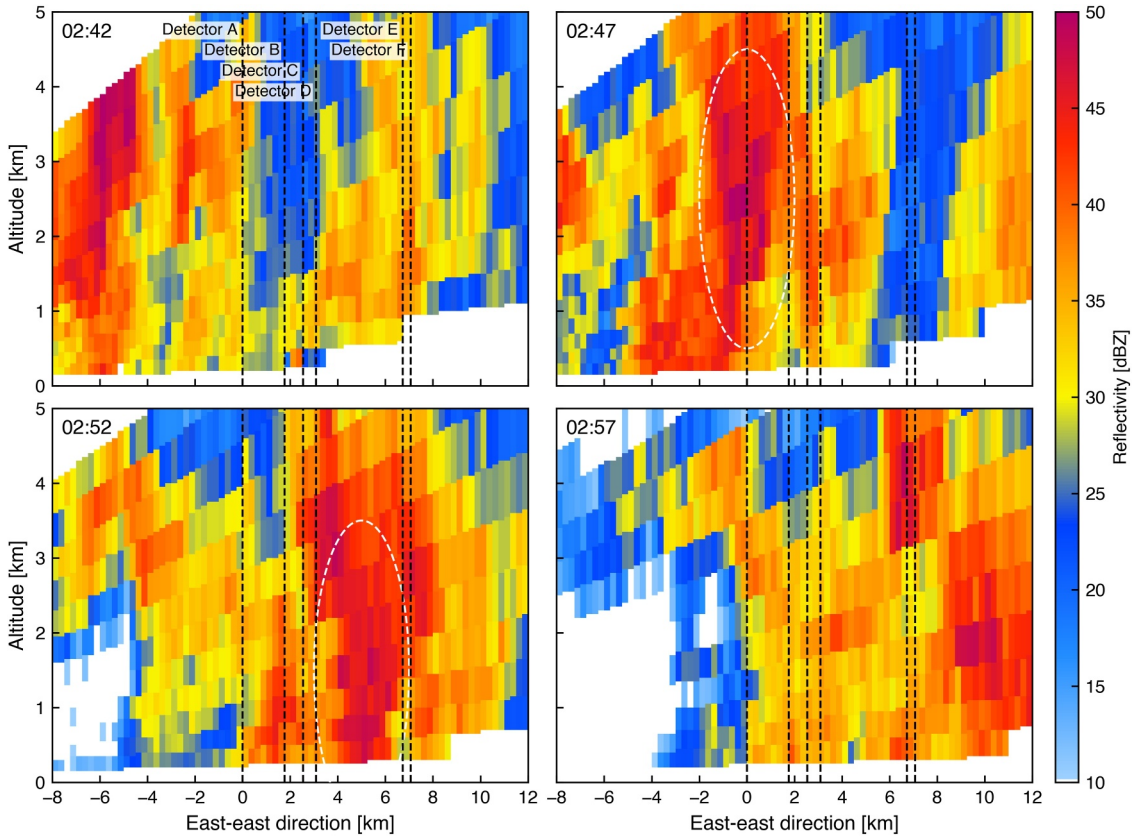

Figure 4. West-east vertical cross sections of reflectivity composited with 12 plan-position indicator (PPI) scans by the Noumi X-band radar. The movement of echoes between the PPI scans is corrected. The north-south positions of the cross sections are shown in Figure 1. The black-dashed lines present the positions of the radiation detectors. The white-dashed eclipses show the descent of the thundercloud core.

respectively. The statistic and systematic errors are 1.0 m s^{-1} and 1.0 m s^{-1}, respectively, and a merged error is 1.5 m s^{-1}.

Figure 4 shows east-west cross sections of the radar echoes obtained by the Noumi X-band radar. These cross sections were created by synthesizing 5-min PPI scans at 12 elevation angles. Taking into account the movement of the radar echoes, the cross sections were corrected to be those at 02:42, 02:47, 02:52, and 02:57. The north-south position of the cross sections was moved along the movement of the radar echoes as shown in Figure 1 so that the cross sections pass through the center of the thundercloud. Due to the limitation of scanning elevation angles, there are unscanned regions in the upper area. At 02:42, a developed radar echo, which seems to have been at the mature stage with strongly vertically developed convection was present at an altitude of 2–4 km southwest of the detector network and the bottom of the echo reached the ground around 02:47. In the cross section at 02:52, the echo can be seen descending further. Detections of gamma-ray glows associated with descending radar echoes have been reported (Wada, Kamogawa, et al., 2023; Wada, Wu, et al., 2023; E. Williams et al., 2022, 2023).

FALMA and DALMA recorded radio-frequency emissions from the lightning discharge from 02:47:16 to 02:47:17. Figure 5 shows the 3D location result obtained with 8 DALMA stations working at this time. The lightning discharge started at 02:47:16.896 at a point 1.7 km west-northwest of Detector A. For the next 40 ms, a vigorous discharge activity was detected at an altitude of less than 1 km around Detector A (within 1.5 km). Furthermore, at around 02:47:16.940, a vertically upward-going leader was observed 1 km northwest of Detector A. This upward leader developed along with the strong echo observed in the west-east cross section obtained by the Noumi X-band radar at 11:47. The lightning discharge lasted for 600 ms. On the other hand, since the discharge activity located by DALMA moved away from Detector A 200 ms after the initiation, only the first 200 ms from 02:47:16.896 are shown in Figure 5 for simplicity.

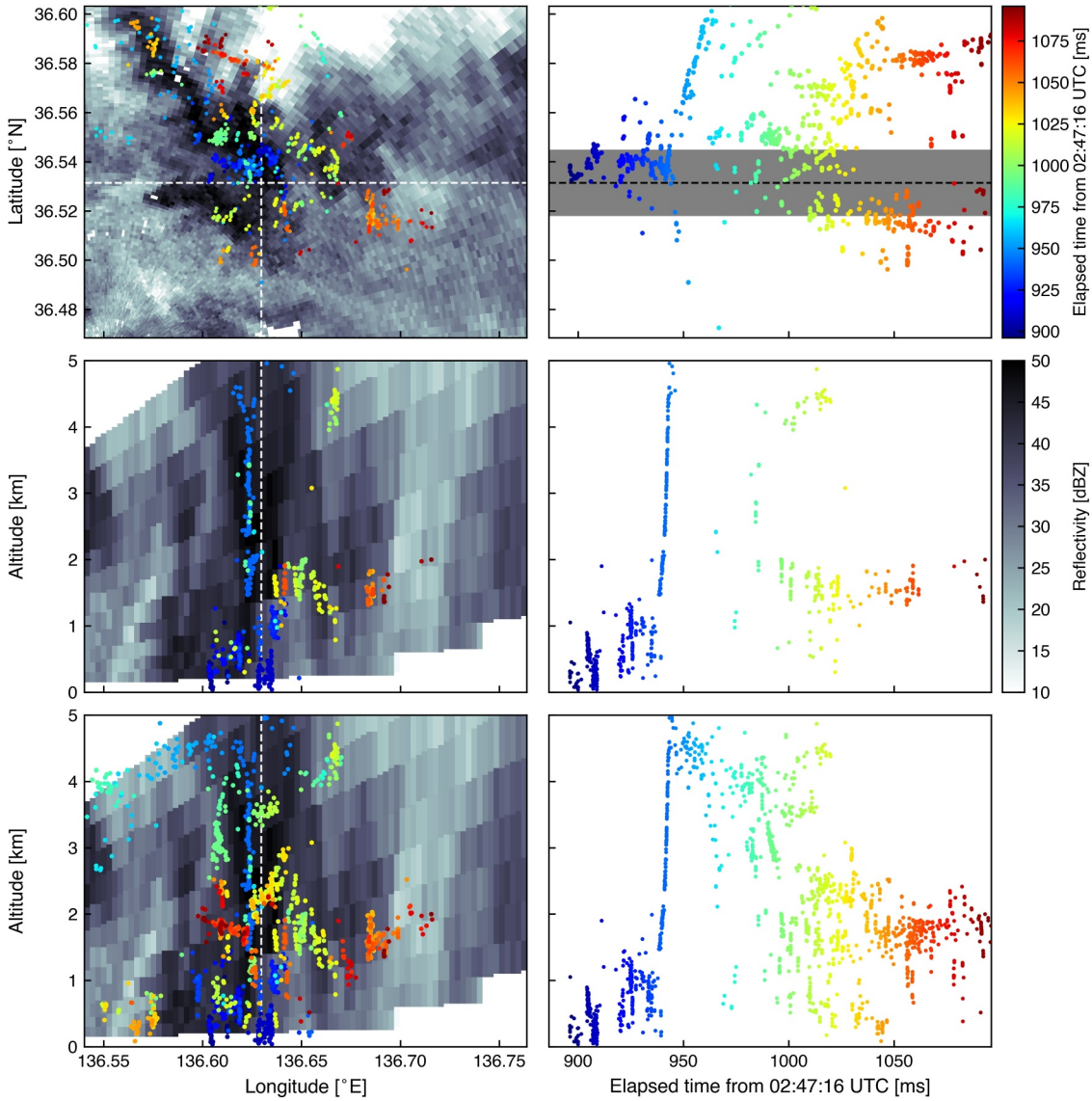

Figure 5. Three-dimensional mapping by DALMA of the lightning discharge terminating the first glow. Left top: Two-dimensional view overlaid with the PPI scan (same as in Figure 3) by the Noumi radar at 02:47. The colors of the markers show the detection time. The white-dashed lines indicate the position of Detector A. Right top: Temporal evolution of the lightning discharge for the north-south direction. The black-dashed line shows the latitude of Detector A (N36.531°). The gray zone indicates the area within 1.5 km from the latitude of Detector A. Left middle: An altitude-longitude view overlaid with the west-east vertical cross section of reflectivity (same as in Figure 4). Only the source locations within 1.5 km from N36.531° (the latitude of Detector A) are presented to emphasize the lightning activity around Detector A. The white-dashed line shows the longitude of Detector A (E136.629°). An upward negative leader is clearly seen in the vicinity of Detector A. Right middle: Temporal evolution of the lightning discharge for the altitude. Only the source locations within 1.5 km from N36.531° are presented. Left bottom and right bottom: the same as the left-middle and right-middle panels but not limited to the sources located within 1.5 km from N36.531°.

4. Discussion

4.1. Comparison Between Gamma-Ray and Radar Observations

The gamma-ray glows were detected from west to east in the order of Detectors A, B, C, and D. The radar echoes detected by the Noumi radar moved from west-southwest to east-northeast, which qualitatively matched the detection order of the gamma-ray glows. Therefore, the gamma-ray glows observed by Detectors B, C, and D are identical, whereas the glow observed by Detector A is another one as it terminated with the lightning discharge before it reached Detector B. Hereafter, the terminated glow recorded by Detector A and the other one by Detectors B, C, and D are called first and second glows, respectively.

The trajectory of the glow center is estimated to be the red-solid line shown in Figure 1 by assuming that (a) the center of the second glow passed over Detector C where the largest count rate was recorded in the detection network, and that (b) the electrified region moved with the thundercloud with the speed and direction of 16.7 ± 1.5 m s^{-1} and 250° respectively, derived from the radar observation. The closest distances to this trajectory for Detectors A, B, D, E, and F are 0.27, 0.07, 0.45, 1.02, and 0.91 km, respectively. This suggests that the center of the second glow could have passed within 100 m of Detector B and offset by several hundred meters to 1 km from Detectors A, D, E, and F.

The distance between the closest point to Detectors A, B, and D on the trajectory and the Detector C is 2.75, 0.84, and 0.44 km. Based on the speed of the thundercloud derived from the radar observation, the region which produced the second glow is expected to have been closest to Detector A at 165 ± 15 s before, Detector B at 50 ± 5 s before, and Detector D at 26 ± 2 s after the peak recorded at Detector C. On the other hand, the termination of the first glow was at 155 s before, and the peak of the second glow recorded by Detectors B and D was at 8.5 ± 1.7 s before and 17.3 ± 1.7 s after derived by fitting the count-rate histories with a Gaussian function. Figure 6 shows the count-rate histories of the glows, the actual peak times, and the expected ones predicted from the movement of the radar echoes. The detection and termination time of the first glow at Detector A is consistent with the expected peak time within the error. Therefore, it is indicative that the first glow and the second glow were produced in the same region of the thundercloud. The detection times at Detectors B and D, however, are not consistent with the expected ones. In particular, the peak time at Detector B is different by ∼40 s from the expected time. These results raise two questions. One is that a gamma-ray glow can be produced in a region of a thundercloud, which seems to be neutralized by a lightning discharge just 2–3 min ago. The other is that an apparent movement of a gamma-ray glow observed by multiple radiation detectors does not necessarily match the movement of thunderclouds.

4.2. Rapid Recovery of Electric Fields

Let us consider the first question. DALMA detected the lightning activity at an altitude of 0.5–1 km (Figure 5), very close to the northwest side of Detector A (within 1 km), within 50 ms of the lightning initiation. Because of the attenuation of gamma rays in the atmosphere, the glow-production region accelerating electrons should be placed near the ground. For example, the mean free path of 1-MeV photons is 122 m and photons are subject to multiple scattering in the atmosphere before reaching the ground. Hence, MeV photons can penetrate several hundred meters in the atmosphere at 1 atm, and it is reasonable to consider that the electron acceleration region that caused the gamma-ray glow existed at an altitude of several hundred meters to 1 km (Wada et al., 2019). Therefore, the discharge activity at low altitude and close range to Detector A is thought to have directly neutralized the electron acceleration region of the first glow leading to the termination.

After the activity at low altitude, an upward leader developed at 0.5–1.5 km northwest of Detector A. Figure 7 shows the time-altitude profile of the lightning discharge obtained by DALMA, and the corresponding broadband LF waveform recorded by one of the FALMA stations at N36.553°, E136.955° (29 km from Detector A). Since active LF emissions associated with the upward leader were recorded in the broadband LF band, not only the low altitude below 1 km but also the upper region at 2–5 km altitude are thought to have been neutralized by the lightning discharge. Most of the broadband LF pulses of the upward leader have a negative onset in the sign convention of the atmospheric electricity. This indicates that this upward leader is a negative one, likely developed from a main negative charge layer, and also suggests that the upper dipole between a main negative and an upper positive charge layers was electrically active. Referring to the initial analysis value at 00:00 UTC of the mesoscale model (MSM) provided by the Japan Meteorological Agency, as shown in the left panel of Figure 7, the −10°C altitude was 1.8 km at which charge separation occurs actively. In addition, as shown in the bottom panels of Figure 7, a lot of radio-frequency sources are located at 1–2-km altitudes by DALMA. These supports that negative charges were accumulated at 1–2 km altitudes. Since the negative upward leader seems to have started around an altitude of 1.5 km, the leader should have discharged an upper main dipole between the main negative and the upper positive charge layers if the conventional tripole structure is considered (E. R. Williams, 1989). Such upward negative leaders between the main negative and upper positive layers have been reported by Yang et al. (2025).

As shown in Figure 4, the developed radar echo at an altitude of 1–3 km at 09:47 moved eastward and descended between 09:47 and 09:52. The echo seems to have been present above Detectors B, C, and D around 09:50 when

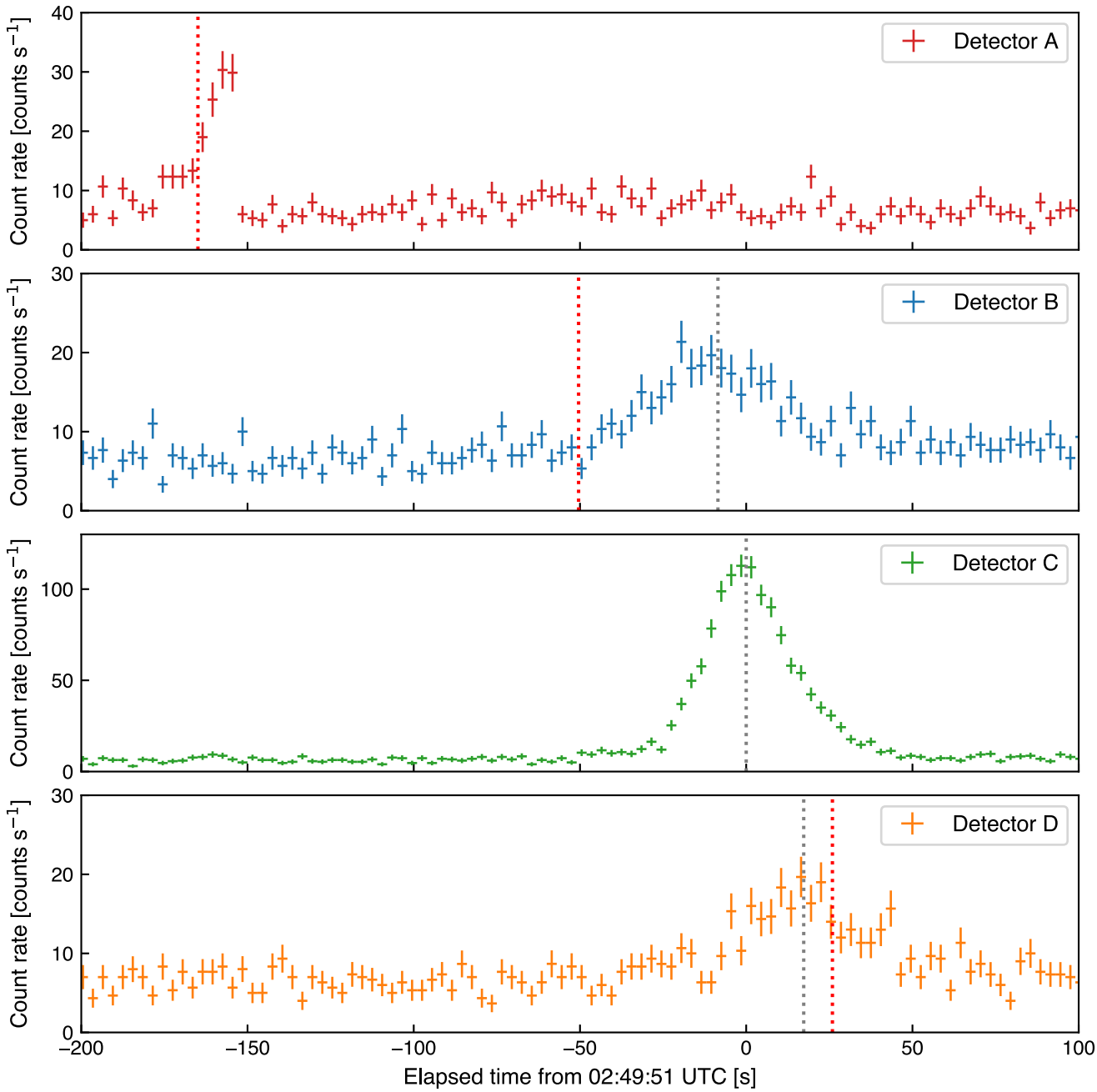

Figure 6. Count-rate histories above 3 MeV recorded by Detectors A, B, C, and D. The gray-dashed lines show the actual peak time of the second glows. The colored-dashed lines show the expected peak time derived from the movement of the radar echo.

the second glow was recorded by those detectors. Since the upward leader of the lightning discharge at 09:47:16 extended toward the developed echo, it is reasonable to consider that the region was (fully or at least partially) neutralized 2–3 min before the detection of the second glow. In particular, the discharge activity seems to have reduced charges in the main negative charge layer.

One of the possible reasons why the second glow was detected after the lightning discharge neutralized the glow-producing region is that a strong electric field was restored within 2–3 min after the lightning discharge. In a situation where strong convection continues, such as in summer thunderclouds, charge separation can occur continuously and the electric field can be restored. In fact, Chilingarian et al. (2020) have reported that TGEs were repeatedly restored even after they were interrupted by lightning discharges. Therefore, active convection may

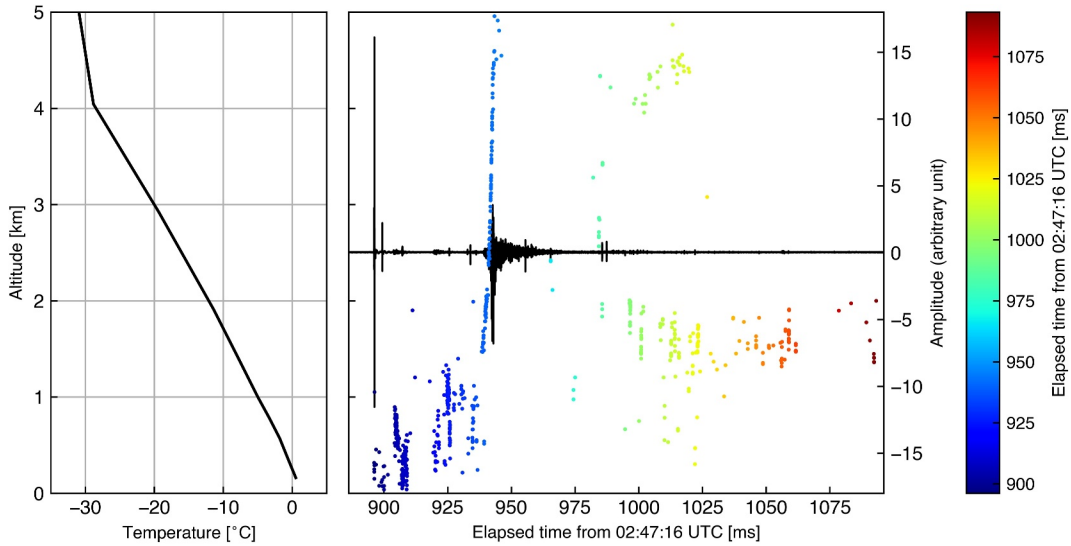

Figure 7. Left: A temperature-altitude profile extracted from the initial analysis data (at 00:00 UTC and N36.5°, E136.625°) of the mesoscale model (MSM) provided by the Japan Meteorological Agency. Right: the time-altitude profile of the lightning discharge obtained by DALMA and the corresponding broadband LF waveform recorded by one of the FALMA stations at N36.553°, E136.955°. Only the source locations within 1.5 km from N36.531° (the latitude of Detector A) are presented in the same way as the bottom-right panel of Figure 5.

cause repeated occurrences of TGEs/gamma-ray glows and interruptions by lightning discharges. On the other hand, convection in winter thunderstorms tends to be less active than in summer ones.

To more closely diagnose the convection in the present case, a Lagrangian analysis was performed. Using the position of Detector C at 02:47 as the reference, a composite of PPIs taken every 5 min was created in a moving coordinate system. The east-west cross section is shown in Figure 8 (the maximum values within 1 km north and south of the reference east-west cross section are extracted). The vertical axis is converted to the corresponding temperature using the MSM temperature profile (the left panel of Figure 7) instead of altitude. At 02:37, no core reaching 50 dBZ was observed at the tracking center, although the maximum observation altitude was limited by the maximum elevation angle because the tracking center was close to the radar at this time. At 02:42, a clear core was observed at the tracking center located between −5°C and −15°C altitude. This core was also clearly seen at 02:47 but showed little movement in the vertical direction. At 02:52, a clear core descent was observed. At 02:57, some precipitation particles remained at the −5°C altitude, but this appears to have almost disappeared by 03:02. Note that another core appeared about 2–3 km west of the target core at 02:52, and it appears to have developed by 02:57 and fallen by 03:02.

As shown above, a clear descent of the thundercloud core was detected from 02:47 to 02:52, when the two glows were detected, and hence the thundercloud is thought to be in the dissipating phase, although it was in the mature stage at 02:42 with strongly vertically developed convection. In the dissipating phase, precipitation particles descend due to weakened updraft, and a difference in descending speed between ice crystals and graupels may cause charge separation. A hypothesis is that separation of graupels and ice crystals associated with descent of the thunderstorm core could have formed a strong electric field in a short time and have produced the second gamma-ray glow, if graupels and ice crystals were in the same region at the moment of the lightning discharge and the charge of the particles was not totally neutralized. In fact, Wada, Enoto et al. (2021) and Wada, Kamogawa, et al. (2023) reported gamma-ray glows in winter thunderstorms associated with graupel precipitation, and also E. Williams et al. (2022) discussed radar observations of graupels associated with TGEs in Armenia.

The surface electric fields recorded by field mills beside Detectors B and D were negative during the second glow (Figure 2), whereas their peaks were not coincident with the count-rate peaks of gamma rays recorded by the radiation detectors. This suggests that a dipole electric field between the main negative charge layer and the ground surface did not produce the second glow. The main negative charge layer can create an upward electric field between the negative charges and positive mirror charges on the surface. This upward field can accelerate

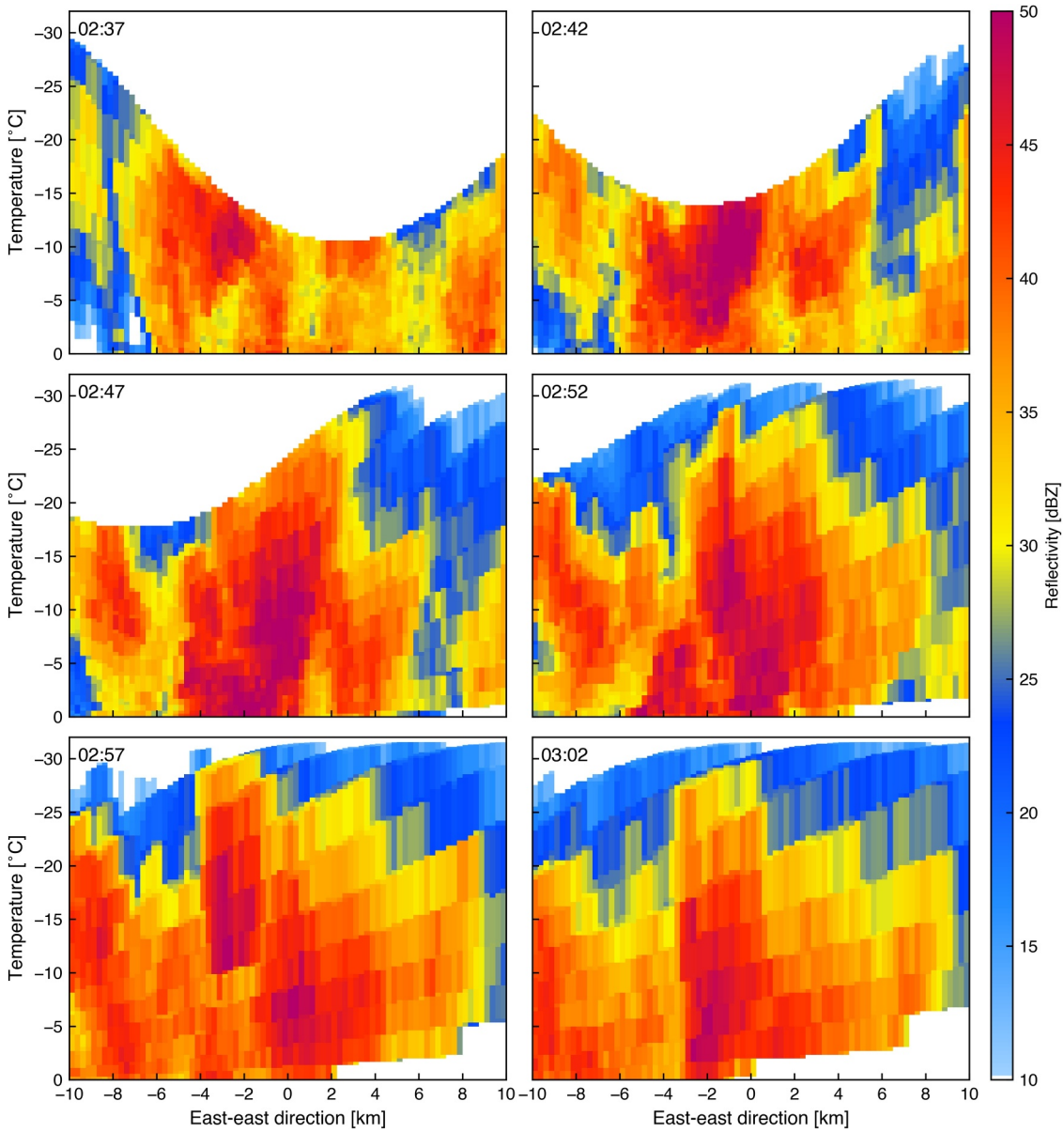

Figure 8. West-east vertical cross sections of reflectivity composited with 12 plan-position indicator (PPI) scans by the Noumi X-band radar in a moving coordinate system with the target thundercloud. The tracking center is set to the location of Detector C at 02:47. The *Y*-axis shows corresponding temperature instead of height. The maximum reflectivity values within 1 km north and south of the reference east-west cross section are extracted.

electrons toward the ground. The strength of the upward electric field directly corresponds to the surface electric field measured by field mills, and gamma-ray glows should be detected at the peak of the electric field. However, this is not the case. Instead, a dipole between the main negative charge and a lower positive charge layers, which could have produced by the rapid separation of graupels and ice crystals, could have contributed to the production of the second glow, as discussed by Wada, Kamogawa, et al. (2023). Even if the lower charge layer exists, the electric field can be negative as the amount of lower positive charges is much smaller than the main negative charges.

4.3. Temporal Variation of Intrinsic Glow Brightness

Let us consider the second question. The second glow observed by Detectors B, C, and D clearly showed peaks in the count rate. However, the peak time did not coincide with the time of closest approach when it was assumed

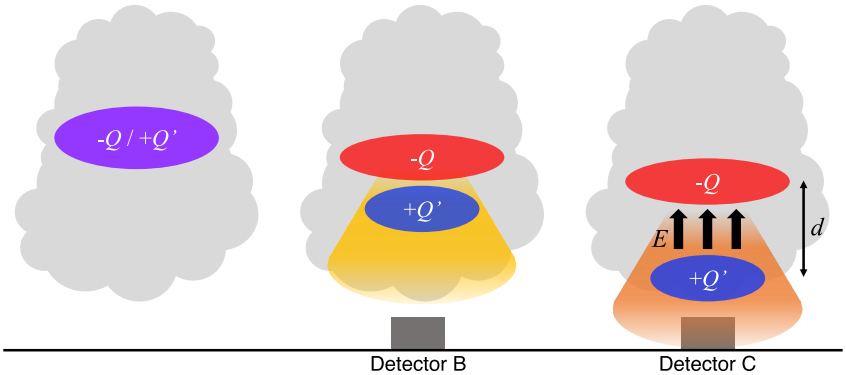

Figure 9. A simplified schematic of the developing electric-field region producing the gamma-ray glow.

that the gamma-ray glowing region moved with the thundercloud cell. This suggests that the intrinsic brightness of the gamma-ray glow was not constant but might have varied over time. As discussed above, it is highly likely that the strong electric field region having produced the second glow developed rapidly within a few minutes after the first glow ceased with the lightning discharge. The second gamma-ray glow may have correspondingly become brighter while passing from Detector B to D especially while passing between B and C. If the gamma-ray glow had brightened after passing over Detector B, this would explain why the peak of the gamma-ray glow recorded by Detector B was delayed from the actual passage of the glowing region.

Also, as shown in Figure 1, the line connecting Detectors B and C is parallel to the direction of movement of the thundercloud. Therefore, when the center of the glowing region passed right above Detector C, it also passed almost right above Detector B. If the intrinsic brightness of the gamma-ray glow on the ground is constant, the peak flux should be roughly the same at Detectors B and C. However, in reality, the peak gamma-ray flux is greater at Detector C than at Detector B. This also supports the hypothesis that the second glow became brighter while it moved from Detector B to C.

Let us consider a very simple model of a parallel plate capacitor to discuss the electric field inside the thundercloud, assuming that there is a lower positive charge layer with graupels, a middle negative charge layer in the center with ice crystals in the thundercloud related to electron acceleration. When the altitude changes in atmospheric pressure are ignored for simplicity, the electric-field strength between the layers E is proportional to the amount of charge in each layer Q, and the voltage between the layers V is proportional to the product of the amount of charge and the distance between the layers d. In other words, when the two charge layers get separated by the different falling speed of precipitation particles, the electric-field strength between the charge layers does not change, but the voltage increases in proportion to the distance. In the RREA model, the number of high-energy electrons (capable of runaway) generated in the strong electric field region, $N(d)$, is expressed as an exponential function of the distance:

$$N(d) = N_0 \exp\left(\frac{eE - F_{\text{th}}}{E_{\text{cut}}} d\right) \quad (1)$$

where N_0 is the number of high-energy seed electrons, e is the elementary charge, $F_{\text{th}} = 0.276$ MeV m^{-1} $\times$ n is the threshold strength of electric field, n is the density of air with respect to that at sea level, and $E_{\text{cut}} = 7.3$ MeV is a representative energy (Dwyer et al., 2012). Namely, as the distance d between the two charge layers increases, the amplification rate of high-energy electrons increases, and as a result, the gamma-ray glow can become brighter. Therefore, it is possible that the difference in the falling speed of the particles caused the brightening of the gamma-ray glow. In a realistic situation, the amount of main negative charges ($-Q$) should be larger than that of lower positive charges ($+Q'$), which is also suggested by the negative trend of the surface electric field. This scenario is explained in Figure 9. Note that it is necessary to take into account the altitude change in atmospheric density, so the amplification rate of high-energy electrons is expected to be more complex (Diniz et al., 2023).

Another factor to consider is the attenuation of high-energy photons by the atmosphere. Since the mean free path of a 1 MeV photon in an atmosphere of 1 atm is 122 m, a proxy of atmospheric attenuation, an atmospheric

Table 1
Summary of Gamma-Ray Glows Reported by Wada, Matsumoto, et al. (2021) That Were Observed by Both Detectors B and D

Detection time (UTC)	Event no.	Wind speed [m s^{-1}]	Wind direction [°]	Actual time interval [s]	Expected time interval [s]
2017-12-25 23:09–23:12	19/20	20.6 ± 1.4	260	56.0 ± 0.7	64 ± 4
2018-12-08 12:08–12:12	36/37	14.0 ± 1.3	250	72.8 ± 6.9	90 ± 8
2018-12-17 14:14–14:18	43/44	11.3 ± 1.3	280	83.3 ± 2.0	116 ± 13
2020-01-12 17:04–17:08	57/58	16.4 ± 1.4	240	43.4 ± 0.7	71 ± 6
2020-02-17 12:48–12:53	62/64	15.0 ± 1.2	250	99.5 ± 3.1	84 ± 7
2020-02-17 12:51–12:55	65/66	15.0 ± 1.2	250	76.5 ± 0.9	84 ± 7

thickness of several hundred meters is critical for the high-energy photons of gamma-ray glows. As shown in Figure 4, the thundercloud core descended by several hundred meters to 1 km in 5 min. Therefore, the descent of the electrified region producing the glow reduced the atmospheric attenuation of high-energy photons and hence increased the flux of gamma rays on the ground surface. The detection of the second glow on the ground surface is therefore supported by a combination of two factors: the increase in accelerated electrons due to the development of the electric-field region and the decrease in atmospheric attenuation of gamma rays between the electrified region and the ground surface due to the descent of the thunderstorm core.

In the present case, no gamma-ray glows were observed by Detectors E and F. Considering the assumed trajectory of the center of the glowing region shown in Figure 1, the region is thought to have been closest to Detectors E and F around 02:54, and in fact, the radar echo passed close to Detectors E and F as shown in Figure 3. However, Detectors E and F are offset by 1.0 and 0.9 km, respectively, from the trajectory of the estimated center of the glowing region. Therefore, even if the gamma-ray glow continued, it may not have been detected due to the offset of the detectors. Also, the thunderstorm core might have reached the ground surface when approaching Detectors E and F (after 02:52), the strong electric field region might have disappeared, and the gamma-ray glow might have ended.

4.4. Revisiting Previous Cases

Based on previous observations, we discuss whether the increase in the intrinsic brightness of the gamma-ray glow in the present case is special or common. Wada, Matsumoto, et al. (2021) have compiled a catalog of 70 cases of gamma-ray glows in winter thunderstorms from October 2016 to March 2020. Among them, there were six cases in which gamma-ray glows were detected simultaneously by Detectors B and D in the present paper and in which the glow peak was observed by both detectors. Table 1 and Figure 10 provide a list and count-rate histories of these cases, respectively. Note that Detector C was not in operation before December 2020. When comparing the time difference of the peaks derived by a Gaussian-function fitting with the expected time difference derived from the wind direction and speed calculated with radar observations, a difference of 10 s or more was observed in four out of six cases. The events on 8 December 2018 (Event 36/37) and 17 February 2020 (Event 62/64) had small gamma-ray fluxes and relatively unclear peaks, and hence it is difficult to conclude that the difference is significant. On the other hand, in particular in the cases of 17 December 2018 (Event 43/44) and 12 January 2020 (Event 57/58), the time difference was significant, 31 and 28 s, respectively. Hisadomi et al. (2021) analyzed the case of 12 January 2020 and discussed the difference between the actual and expected peaks of the count rate. In these events, the gamma-ray flux on the ground may have increased due to the development and/or descent of a strong electric-field region while passing between the two points. Therefore, the present case is not unique, and it is possible that the intrinsic brightness of gamma-ray glows may change during observations at the two points.

5. Conclusion

We reported two successive gamma-ray glows tracked by four radiation detectors. The first one was recorded only by Detector A and was quenched by the lightning discharge. The second was tracked by Detectors B, C, and D 2–3 min after the termination of the first glow. The radar observations reveal that both glows were generated in the same thundercloud core. On the other hand, the lightning discharge that terminated the first glow seems to have neutralized electric fields in the thundercloud core. The tracking observation of the second glow provided the time

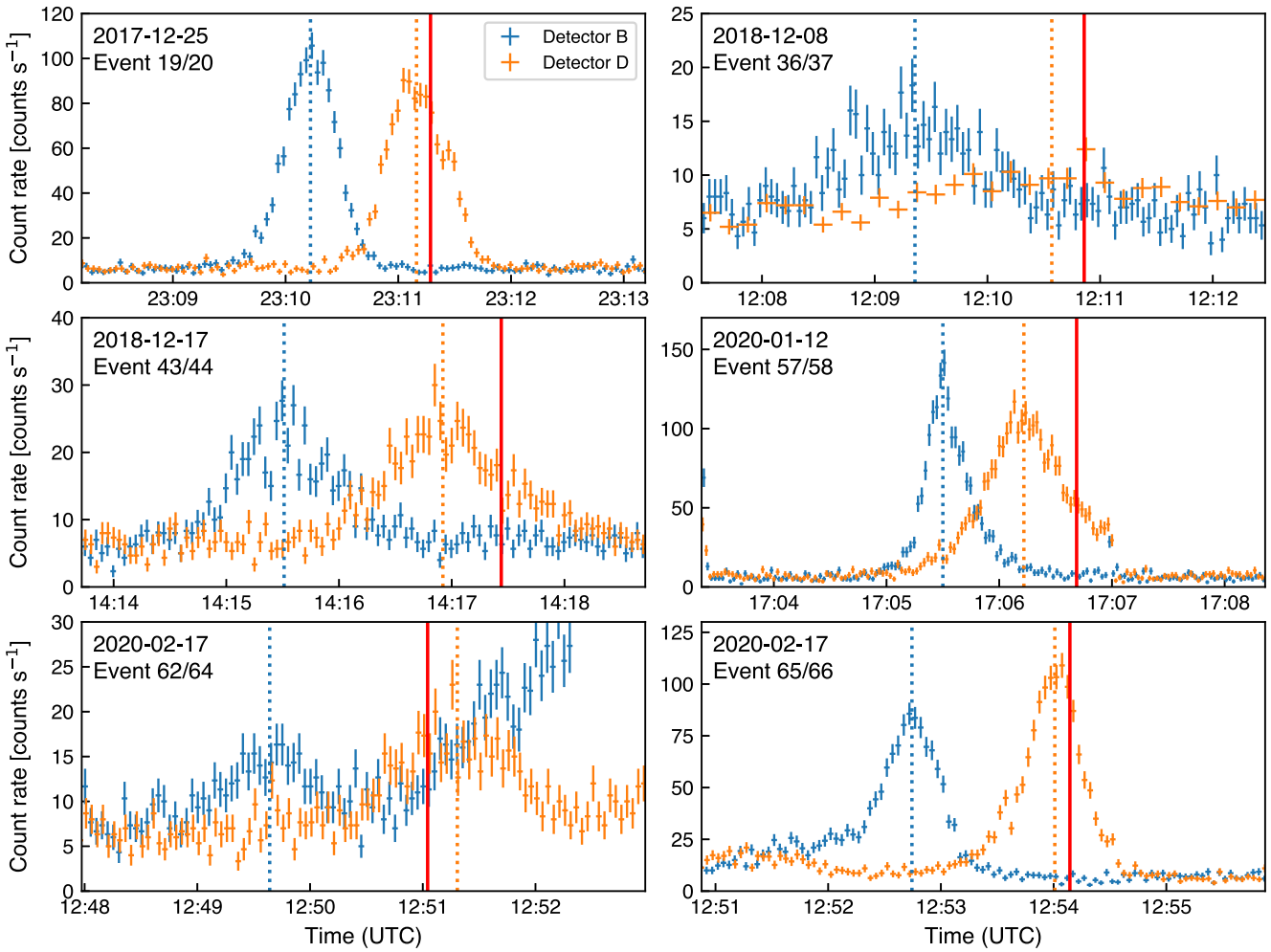

Figure 10. Count-rate histories of gamma-ray glows reported by Wada, Matsumoto, et al. (2021) that were observed by both Detectors B and D. Blue and orange dashed lines indicate the peak time of the count-rate histories recorded by Detectors B and D, respectively. The red-solid lines show the expected peak time derived from the wind speed and direction.

of count-rate peaks. However, the peak timing was not consistent with the expected one from the thundercloud movement derived from the radar observations.

Based on the observations, we raised two questions; one is how the electric field that generated the second glow recovered from the lightning discharge in 2–3 min. The other one is how to explain the discrepancy between an apparent movement of the gamma-ray glow observed by multiple radiation detectors and the movement of the thundercloud. Our result indicates that the descent of the thundercloud core may have contributed to the quick recovery of the electric field and the brightening of the second glow. Different precipitation particles have different falling speeds and charge polarities. During the descent of the thundercloud core, two charge layers with opposite polarities may have gotten separated, and electron acceleration and multiplication for the second glow may have been strengthened above Detector C as the electric-field region gained enough length for the electron avalanches. Several gamma-ray glows at the same places previously reported by Wada, Matsumoto, et al. (2021) and Hisadomi et al. (2021) show the same discrepancy, and the rapid brightening of gamma-ray glows above radiation detectors is not a special case. Detecting gamma-ray glows only with one sensor cannot distinguish the temporal development of glows, and hence tracking observations with multiple sensors are necessary to understand the development and the lifecycle of gamma-ray glows.

Conflict of Interest

The authors declare no conflicts of interest relevant to this study.

Data Availability Statement

The materials used in this study can be found online (Wada, 2025). The materials of Wada, Matsumoto, et al. (2021) can also be found online (Wada, 2021). The XRAIN data are provided on the Data Integration and Analysis System (DIAS: https://diasjp.net/en/app_list/xrain-data/) upon registration. The MSM data are provided by the Japan Meteorological Agency via Research Institute for Sustainable Humanosphere, Kyoto University (http://database.rish.kyoto-u.ac.jp/arch/jmadata/data/gpv/original/).

Acknowledgments
The $Be_4Ge_3O_{12}$ scintillation crystal of the present study is provided by Dr. H. Sakurai and Dr. M. Niikura. We thank Dr. K. Watarai at Kanazawa University High School, Mr. Kenta Ikawa at Kanazawa Izumigaoka High School, Mr. Takaaki Kouen and Mr. Koichiro Kimura at Kanazawa Nisui High School, and Mr. Hideaki Okamura at Kanazawa Institute of Technology for the support of detector deployment. This research is supported by JSPS/MEXT KAKENHI Grants 21H01116, 22K14453, 24H00257, 24H00269, and 25K01013. GSD is supported by the FAPESP project 2024/10417-0.

References

Brook, M., Nakano, M., Krehbiel, P., & Takeuti, T. (1982). The electrical structure of the Hokuriku winter thunderstorms. *Journal of Geophysical Research*, *87*(C2), 1207–1215. https://doi.org/10.1029/jc087ic02p01207

Chilingarian, A., Daryan, A., Arakelyan, K., Hovhannisyan, A., Mailyan, B., Melkumyan, L., et al. (2010). Ground-based observations of thunderstorm-correlated fluxes of high-energy electrons, gamma rays, and neutrons. *Physical Review D*, *82*(4), 043009. https://doi.org/10.1103/physrevd.82.043009

Chilingarian, A., Hovsepyan, G., & Vanyan, L. (2014). On the origin of the particle fluxes from the thunderclouds: Energy spectra analysis. *EPL*, *106*(5), 59001. https://doi.org/10.1209/0295-5075/106/59001

Chilingarian, A., Khanikyants, Y., Mareev, E., Pokhsraryan, D., Rakov, V. A., & Soghomonyan, S. (2017). Types of lightning discharges that abruptly terminate enhanced fluxes of energetic radiation and particles observed at ground level. *Journal of Geophysical Research: Atmospheres*, *122*(14), 7582–7599. https://doi.org/10.1002/2017jd026744

Chilingarian, A., Khanikyants, Y., Rakov, V., & Soghomonyan, S. (2020). Termination of thunderstorm-related bursts of energetic radiation and particles by inverted intracloud and hybrid lightning discharges. *Atmospheric Research*, *233*, 104713. https://doi.org/10.1016/j.atmosres.2019.104713

Chilingarian, A., Mailyan, B., & Vanyan, L. (2012). Recovering of the energy spectra of electrons and gamma rays coming from the thunderclouds. *Atmospheric Research*, *114–115*, 1–16. https://doi.org/10.1016/j.atmosres.2012.05.008

Chilingarian, A., & Mkrtchyan, H. (2012). Role of the lower positive charge region (lpcr) in initiation of the thunderstorm ground enhancements (tges). *Physical Review D*, *86*(7), 072003. https://doi.org/10.1103/physrevd.86.072003

Chilingarian, A., Mkrtchyan, H., Karapetyan, G., Chilingaryan, S., Sargsyan, B., & Arestakesyan, A. (2019). Catalog of 2017 thunderstorm ground enhancement (tge) events observed on aragats. *Scientific Reports*, *9*(1), 6253. https://doi.org/10.1038/s41598-019-42786-7

Chum, J., Langer, R., Baše, J., Kollárik, M., Strhárský, I., Diendorfer, G., & Rusz, J. (2020). Significant enhancements of secondary cosmic rays and electric field at the high mountain peak of lomnický štít in high tatras during thunderstorms. *Earth Planets and Space*, *72*(1), 28. https://doi.org/10.1186/s40623-020-01155-9

Cramer, E. S., Mailyan, B. G., Celestin, S., & Dwyer, J. R. (2017). A simulation study on the electric field spectral dependence of thunderstorm ground enhancements and gamma ray glows. *Journal of Geophysical Research: Atmospheres*, *122*(9), 4763–4772. https://doi.org/10.1002/2016jd026422

Diniz, G. S., Wada, Y., Ohira, Y., Nakazawa, K., Tsurumi, M., & Enoto, T. (2023). Relativistic runaway electron avalanche development near the electric field threshold in inhomogeneous air. *Geophysical Research Letters*, *50*(20), e2023GL105087. https://doi.org/10.1029/2023gl105087

Dwyer, J. R. (2003). A fundamental limit on electric fields in air. *Geophysical Research Letters*, *30*(20), 2055. https://doi.org/10.1029/2003gl017781

Dwyer, J. R. (2012). The relativistic feedback discharge model of terrestrial gamma ray flashes. *Journal of Geophysical Research*, *117*(A2), A02308. https://doi.org/10.1029/2011ja017160

Dwyer, J. R., Smith, D. M., & Cummer, S. A. (2012). High-energy atmospheric physics: Terrestrial gamma-ray flashes and related phenomena. *Space Science Reviews*, *173*(1–4), 133–196. https://doi.org/10.1007/s11214-012-9894-0

Eack, K. B., & Beasley, W. H. (2015). Long-duration x-ray emissions observed in thunderstorms. *Journal of Geophysical Research: Atmospheres*, *120*(14), 6887–6897. https://doi.org/10.1002/2015jd023262

Eack, K. B., Beasley, W. H., Rust, W. D., Marshall, T. C., & Stolzenburg, M. (1996). Initial results from simultaneous observation of x-rays and electric fields in a thunderstorm. *Journal of Geophysical Research*, *101*(D23), 29637–29640. https://doi.org/10.1029/96jd01705

Eack, K. B., Suszcynsky, D. M., Beasley, W. H., Roussel-Dupre, R., & Symbalisty, E. (2000). Gamma-ray emissions observed in a thunderstorm anvil. *Geophysical Research Letters*, *27*(2), 185–188. https://doi.org/10.1029/1999gl010849

Gurevich, A., Milikh, G., & Roussel-Dupre, R. (1992). Runaway electron mechanism of air breakdown and preconditioning during a thunderstorm. *Physics Letters A*, *165*(5–6), 463–468. https://doi.org/10.1016/0375-9601(92)90348-p

Gurevich, A. V., & Zybin, K. P. (2001). Runaway breakdown and electric discharges in thunderstorms. *Physics-Uspekhi*, *44*(11), 1119–1140. https://doi.org/10.1070/pu2001v044n11abeh000939

Hisadomi, S., Nakazawa, K., Wada, Y., Tsuji, Y., Enoto, T., Shinoda, T., et al. (2021). Multiple gamma-ray glows and a downward TGF observed from nearby thunderclouds. *Journal of Geophysical Research: Atmospheres*, *126*(18), e2021JD034543. https://doi.org/10.1029/2021jd034543

Kelley, N. A., Smith, D. M., Dwyer, J. R., Splitt, M., Lazarus, S., Martinez-McKinney, F., et al. (2015). Relativistic electron avalanches as a thunderstorm discharge competing with lightning. *Nature Communications*, *6*(1), 7845. https://doi.org/10.1038/ncomms8845

Kitagawa, N. (1992). Charge distribution of winter thunderclouds. *Res. Lett. Atmos. Electr.*, *12*(2), 143–153. https://doi.org/10.1541/jae.12.143

Kitagawa, N., & Michimoto, K. (1994). Meteorological and electrical aspects of winter thunderclouds. *Journal of Geophysical Research*, *99*(D5), 10713. https://doi.org/10.1029/94jd00288

Kochkin, P., Sarria, D., Lehtinen, N., Mezentsev, A., Yang, S., Genov, G., et al. (2021). A rapid gamma-ray glow flux reduction observed from 20 km altitude. *Journal of Geophysical Research: Atmospheres*, *126*(9), e2020JD033467. https://doi.org/10.1029/2020jd033467

Kochkin, P., van Deursen, A. P. J., Marisaldi, M., Ursi, A., de Boer, A. I., Bardet, M., et al. (2017). In-flight observation of gamma ray glows by ildas. *Journal of Geophysical Research: Atmospheres*, *122*(23), 12801–12811. https://doi.org/10.1002/2017jd027405

Kudela, K., Chum, J., Kollárik, M., Langer, R., Strhárský, I., & Baše, J. (2017). Correlations between secondary cosmic ray rates and strong electric fields at lomnický štít. *Journal of Geophysical Research: Atmospheres*, *122*(20), 10700–10710. https://doi.org/10.1002/2016jd026439

Kuroda, Y., Oguri, S., Kato, Y., Nakata, R., Inoue, Y., Ito, C., & Minowa, M. (2016). Observation of gamma ray bursts at ground level under the thunderclouds. *Physics Letters B*, *758*, 286–291. https://doi.org/10.1016/j.physletb.2016.05.029

Maesaka, T., Maki, M., Iwanami, K., Tsuchiya, S., Kieda, K., & Hoshi, A. (2011). Operational rainfall estimation by x-band mp radar network in mlit, Japan. In *35th conference on radar meteorology*.

Marisaldi, M., Østgaard, N., Mezentsev, A., Lang, T., Grove, J. E., Shy, D., et al. (2024). Highly dynamic gamma-ray emissions are common in tropical thunderclouds. *Nature*, *634*(8032), 57–60. https://doi.org/10.1038/s41586-024-07936-6

McCarthy, M., & Parks, G. K. (1985). Further observations of x-rays inside thunderstorms. *Geophysical Research Letters*, *12*(6), 393–396. https://doi.org/10.1029/gl012i006p00393

Michimoto, K. (1991). A study of radar echoes and their relation to lightning discharge of thunderclouds in the hokuriku district. *Journal of the Meteorological Society of Japan. Series II*, *69*(3), 327–336. https://doi.org/10.2151/jmsj1965.69.3_327

Michimoto, K. (1993). A study of radar echoes and their relation to lightning discharges of thunderclouds in the Hokuriku district. *Journal of the Meteorological Society of Japan. Series II*, *71*(2), 195–204. https://doi.org/10.2151/jmsj1965.71.2_195

Østgaard, N., Christian, H., Grove, J., Sarria, D., Mezentsev, A., Kochkin, P., et al. (2019). Gamma-ray glow observations at 20 km altitude. *Journal of Geophysical Research: Atmospheres*, *124*(13), 7236–7254. https://doi.org/10.1029/2019jd030312

Parks, G. K., Mauk, B. H., Spiger, R., & Chin, J. (1981). X-ray enhancements detected during thunderstorm and lightning activities. *Geophysical Research Letters*, *8*(11), 1176–1179. https://doi.org/10.1029/gl008i011p01176

Torii, T., Sugita, T., Kamogawa, M., Watanabe, Y., & Kusunoki, K. (2011). Migrating source of energetic radiation generated by thunderstorm activity. *Geophysical Research Letters*, *38*(24). https://doi.org/10.1029/2011gl049731

Torii, T., Takeishi, M., & Hosono, T. (2002). Observation of gamma-ray dose increase associated with winter thunderstorm and lightning activity. *Journal of Geophysical Research*, *107*(D17), ACL2-1–ACL2-13. https://doi.org/10.1029/2001jd000938

Tsuchiya, H., Enoto, T., Iwata, K., Yamada, S., Yuasa, T., Kitaguchi, T., et al. (2013). Hardening and termination of long-duration γ rays detected prior to lightning. *Physical Review Letters*, *111*(1), 015001. https://doi.org/10.1103/physrevlett.111.015001

Tsuchiya, H., Enoto, T., Yamada, S., Yuasa, T., Kawaharada, M., Kitaguchi, T., et al. (2007). Detection of high-energy gamma rays from winter thunderclouds. *Physical Review Letters*, *99*(16), 165002. https://doi.org/10.1103/physrevlett.99.165002

Tsuchiya, H., Enoto, T., Yamada, S., Yuasa, T., Nakazawa, K., Kitaguchi, T., et al. (2011). Long-duration γ ray emissions from 2007 and 2008 winter thunderstorms. *Journal of Geophysical Research*, *116*(D9), D09113. https://doi.org/10.1029/2010jd015161

Tsurumi, M., Enoto, T., Ikkatai, Y., Wu, T., Wang, D., Shinoda, T., et al. (2023). Citizen science observation of a gamma-ray glow associated with the initiation of a lightning flash. *Geophysical Research Letters*, *50*(13), e2023GL103612. https://doi.org/10.1029/2023gl103612

Wada, Y., Tsurumi, M., Hayashi, S., & Michimoto, K. (2023). Synoptic meteorological conditions of gamma-ray glows in winter thunderstorms. *Progress in Earth and Planetary Science*, *10*(1), 6. https://doi.org/10.1186/s40645-023-00538-2

Wada, Y. (2021). *Materials for catalog of gamma-ray glows during four winter seasons in Japan*. Mendeley. https://doi.org/10.17632/NRTMMBX3JG.1

Wada, Y. (2025). Materials for rapid recharge and descent of thundercloud core producing gamma-ray glow [Dataset]. *Mendeley*. https://doi.org/10.17632/47njks8z3w.1

Wada, Y., Bowers, G. S., Enoto, T., Kamogawa, M., Nakamura, Y., Morimoto, T., et al. (2018). Termination of electron acceleration in thundercloud by intracloud/intercloud discharge. *Geophysical Research Letters*, *45*(11), 5700–5707. https://doi.org/10.1029/2018gl077784

Wada, Y., Enoto, T., Kubo, M., Nakazawa, K., Shinoda, T., Yonetoku, D., et al. (2021). Meteorological aspects of gamma-ray glows in winter thunderstorms. *Geophysical Research Letters*, *48*(7), e2020GL091910. https://doi.org/10.1029/2020gl091910

Wada, Y., Enoto, T., Nakamura, Y., Furuta, Y., Yuasa, T., Nakazawa, K., et al. (2019). Gamma-ray glow preceding downward terrestrial gamma-ray flash. *Communications Physics*, *2*(1), 67. https://doi.org/10.1038/s42005-019-0168-y

Wada, Y., Kamogawa, M., Kubo, M., Enoto, T., Hayashi, S., Sawano, T., et al. (2023). Negative excursion of surface electric fields during gamma-ray glows in winter thunderstorms. *Journal of Geophysical Research: Atmospheres*, *128*(21), e2023JD039354. https://doi.org/10.1029/2023jd039354

Wada, Y., Matsumoto, T., Enoto, T., Nakazawa, K., Yuasa, T., Furuta, Y., et al. (2021). Catalog of gamma-ray glows during four winter seasons in Japan. *Physical Review Research*, *3*(4), 043117. https://doi.org/10.1103/physrevresearch.3.043117

Wada, Y., Wu, T., Wang, D., Enoto, T., Nakazawa, K., Morimoto, T., et al. (2023). Termination of downward-oriented gamma-ray glow by normal-polarity in-cloud discharge activity. *Journal of Geophysical Research: Atmospheres*, *128*(15), e2023JD038606. https://doi.org/10.1029/2023jd038606

Wang, D., Wu, T., Huang, H., Yang, J., & Yamamoto, K. (2022). 3D mapping of winter lightning in Japan with an array of discone antennas. *IEEJ Transactions on Electrical and Electronic Engineering*, *17*(11), 1606–1612. https://doi.org/10.1002/tee.23667

Williams, E., Mailyan, B., Karapetyan, G., & Mkrtchyan, H. (2023). Conditions for energetic electrons and gamma rays in thunderstorm ground enhancements. *Journal of Geophysical Research: Atmospheres*, *128*(24), e2023JD039612. https://doi.org/10.1029/2023jd039612

Williams, E., Mkrtchyan, H., Mailyan, B., Karapetyan, G., & Hovakimyan, S. (2022). Radar diagnosis of the thundercloud electron accelerator. *Journal of Geophysical Research: Atmospheres*, *127*(11), e2021JD035957. https://doi.org/10.1029/2021jd035957

Williams, E. R. (1989). The tripole structure of thunderstorms. *Journal of Geophysical Research*, *94*(D11), 13151–13167. https://doi.org/10.1029/jd094id11p13151

Wu, T., Wang, D., & Takagi, N. (2018). Lightning mapping with an array of fast antennas. *Geophysical Research Letters*, *45*(8), 3698–3705. https://doi.org/10.1002/2018gl077628

Yang, Q., Wang, D., Wu, T., Smith, D. M., Wada, Y., Nakazawa, K., & Kamogawa, M. (2025). Typical winter tgf lightning: Vertical negative leader progression features and charge structures. *Geophysical Research Letters*, *52*(17), e2024GL114087. https://doi.org/10.1029/2024gl114087

Yuasa, T., Wada, Y., Enoto, T., Furuta, Y., Tsuchiya, H., Hisadomi, S., et al. (2020). Thundercloud project: Exploring high-energy phenomena in thundercloud and lightning. *Progress of Theoretical and Experimental Physics*, *2020*(10), 103H01. https://doi.org/10.1093/ptep/ptaa115